Green energy based inductive Self-Healing highways of the future

Prasanth, Venugopal; Scheele, Natalia; Visser, Erwin; Shekhar, Aditya; Chandra Mouli, Gautham Ram; Bauer, Pavol; Silvester, Sacha

DOI
10.1109/ITEC.2016.7520268

Publication date
2016

Document Version
Accepted author manuscript

Published in
2016 IEEE Transportation Electrification Conference and Expo, ITEC 2016

Green Energy based Inductive Self-Healing Highways of the Future

Venugopal Prasanth, Natalia Scheele, Erwin Visser, Aditya Shekhar, Gautham Ram Chandra Mouli, Pavol Bauer, Sacha Silvester
Delft University of Technology (TU Delft)
The Netherlands
Email: v.prasanth@tudelft.nl, a.shekhar@tudelft.nl, p.bauer@tudelft.nl, s.silvester@tudelft.nl

***Abstract*—This paper deals with a green energy highway in the Netherlands. Here, the development of electric mobility and self-driving cars is introduced. The ideas of wireless power integration with green energy technologies - solar and wind is considered. In case of wind energy, conventional turbines and bladeless vortex are considered as options. Solaroads along the emergency lanes are also investigated. A Dutch highway A12 is considered as a case study and sizing of these energy sources for electric mobility is considered. A grid power demand profile is considered and number of EVs that can be charged hourly is calculated. A preliminary investigation of the combination of IPT and Self-Healing roads is considered in this study.**

I. Introduction

The highway of the future is expected to perform three major operations so as to accommodate a transitory scenario to full electric mobility. These functions include energy generation, energy transport to the electric vehicles (EV) with a large fleet of autonomous vehicles and low maintenance self-healing roads based on inductive heating. Such a green energy highway concept is shown in Fig. 1.

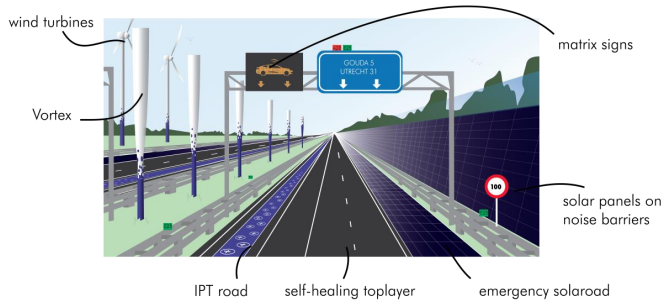

Fig. 1. A green energy Dutch highway integrating wind energy (eg: turbines, vortex), solar energy (Solaroads and solar panels on the noise barrier), IPT enabled roads with self-healing asphalt and Electric Vehicles.

The four different technologies that can enable such a vision with power electronics, electrical machinery and material sciences as the framework are:

- Electric Vehicle and More Autonomous Vehicles
- Wireless Inductive Power Transfer (IPT) for EVs
- Green Energy Technologies (Wind and Solar based on Vortex and SolaRoad)
- Self-Healing Material based Roads

A. Electric Vehicles and More Autonomous Vehicles

Traditional utilization of fossil fuels propelled the industrialization of world and created an era of economic and human prosperity. In addition, the fact that fossil fuels are getting depleted at a very fast rate and its impact on the environment - global warming, climate change, pollution and resulting ecological destruction demands a shift to alternative modes of generation and utilization [1]. According to ITF (International Transport Forum) 2010 statistics, transportation accounted for 23% of the total CO_2 emissions and 30% of OECD CO_2 emissions [2]. Also, it is reported to account for about 15% of the total GHG emissions.

The efficacy of EVs as a solution to the problem is notable as it produces no CO_2 emissions, it does not pollute the environment and is relatively silent. Among EU countries, Norway and the Netherlands are front runners in terms of sales of EVs in 2014 [3]. A major goal for the Netherlands is to add a million EVs by 2025 [3]. Another technological progress is the innovation toward autonomy of vehicles. A description of the autonomy level and its introduction in the market is depicted in Fig. 2.

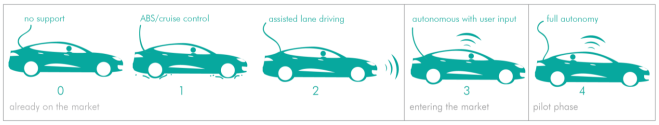

Fig. 2. The different levels of automation. Level 1 to 3 are available for consumers. Level 4 is still in the test phase and the Dutch law does not allow consumers to drive around in this type of vehicle.

These different levels of autonomy to vehicles are defined by the NHTSA (National Highway Traffic Safety Administration) [4] as:

- Level 1 *Function-Specific Automation*, control function that are specific such as cruise control, lane guidance and automated parallel parking.
- Level 2 *Combined Function Automation*, where multiple function specific control integrated such as adaptive cruise control with lane centering.
- Level 3 *Limited Self-Driving Automation*, where all safety critical functions are automated (steering wheel, throttle,

brake). In such an implementation, drivers are not expected to constantly monitor the roadway,

- Level 4 *Full Self-Driving Automation*, all safety critical driving functions are automated and monitoring of roadway is also automated. In such a case, occupants may/may not know driving.

Level 0 is when there exists no autonomy at all. The expectation of automation technology is that in the Netherlands, among various scenarios of technology improvement and policy scenario, the levels of automated vehicles will vary from 1 and 11% in 2030 and between 7% and 61% in 2050 [5].

B. Wireless Inductive Power Transfer for EVs

Inductive Power Transfer involves the transfer of power from a coil to another displaced over an air-gap. The operating principle involves the generation of an alternating magnetic field from an ac supply (*Ampere's law*). Such an alternating field when linked with another coil induces an emf (*Faraday-Lenz law of induction*). The disadvantage of an incipient large air-gap is the large reluctance it adds to the magnetic path. Thus, compensating capacitors are added to both the coils which are then tuned to resonance so as to nullify the reactive power [6]. This technology that eliminates wired power transfer is called Wireless Power Transfer. A typical IPT system based EV is shown in Fig. 3.

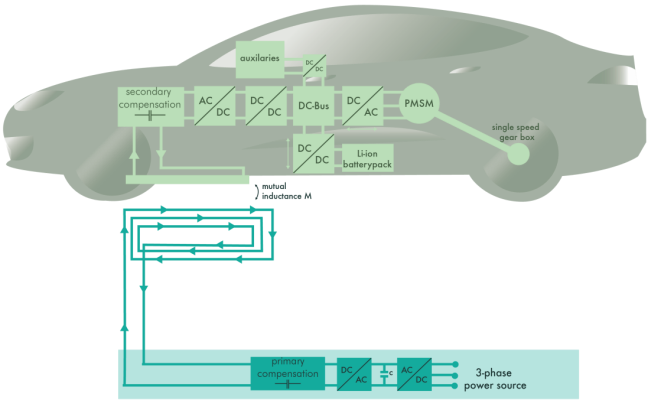

Fig. 3. A typical IPT system with a 3-phase power source that drives an EV with a PMSM machine. Different configurations can have a 1-phase ac, 3-phase ac or even a dc power input source. Also, depending on the EV, the e-Powertrain will change.

Due to its reliance on magnetic fields, this is called Inductive Power Transfer (IPT). There are a number of essential system requirements for an IPT system, they are [7]:

- *Coil magnetics*: A pair of coils that can transfer power from the ground to EV. Usually, a coil based on copper, ferrites (field shaping) and magnetic shield (Al) forms the charge pad (concentrated IPT system) or it can be in the form of long tracks for distributed IPT systems.
- *Power inverter*, where ac is generated in the VLF (3 – 30 kHz)/LF (30 – 300 kHz) frequency range with embedded primary power-control.
- *Energy Management*, typically consisting of a DC/DC converter with control so as to perform secondary power-control to the vehicle battery.

C. Green Energy Technologies

In the Netherlands, solar and wind energy are considered the major sources for highway based energy generation [8]. While conventional technologies can be installed, in this paper we also consider two revolutionary technologies that have vast untapped potential:

- Bladeless Vortex [9]
- SolaRoads [10]

1) Bladeless Vortex: Bladeless vortex is a Spanish technology startup that produces turbines without blades that harness the *'vorticity'* of wind through the fibre glass and carbon fibre cylindrical structure [9]. Thus, the structure uses shear force of the wind that when falling onto the structure creates *eddies* [11]. This reciprocation is converted into electrical energy by cutting a magnetic field produced by magnets in the base. Due to the lack of blades, it has no friction and has no gears and hence reduced maintenance. Also, it is considerably cheaper. A figure showing a prototype of the same (Vortex Mini) and its performance characteristics is presented in Fig. 4 [9].

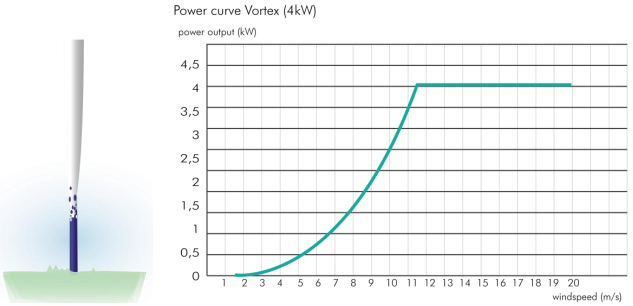

Fig. 4. A 4-kW Vortex and its power-velocity profile, this turbine has a minimum safety distance of 13m from each other [9]

Some disadvantages of this technology include low efficiency, low power outputs thus far, viability for scaling up (stability of structure) and noise. However, the technology due to its cost-effective nature is a good solution for highways. This also considering places where land is limited for large sized classical propeller turbines due to existing infrastructure.

2) Solaroads: Solaroads is a Dutch innovation (TNO, Provence of Noord-Holland, Dynniq and Ooms Civiel) in which prefabricated concrete modules are laid on the ground [10]. On top of this, a layer of tempered glass that is translucent to light is used to absorb light and convert to electricity using crystalline silicon solar cells. A detailed analysis of Solaroads has been carried out in [12]. The maximum module efficiency attained from the study is 9.69%. Some important performance parameters are presented in Fig. 5.

D. Self-Healing Material based Roads

Typically roads are made of porous asphalt concrete in the Netherlands. Porous asphalt concrete has advantages over

dense graded asphalt concrete with respect to noise reduction and water drainage. However the porous structure does not benefit from the durability of asphalt and will cause premature raveling of the road [13]. Asphalt concrete is a self-healing material [14]. Micro cracks are formed in the material when it is exposed to a sufficiently large stress or strain. The self-healing (molecular rearrangement) process will start after the load that generated the damage has been removed.

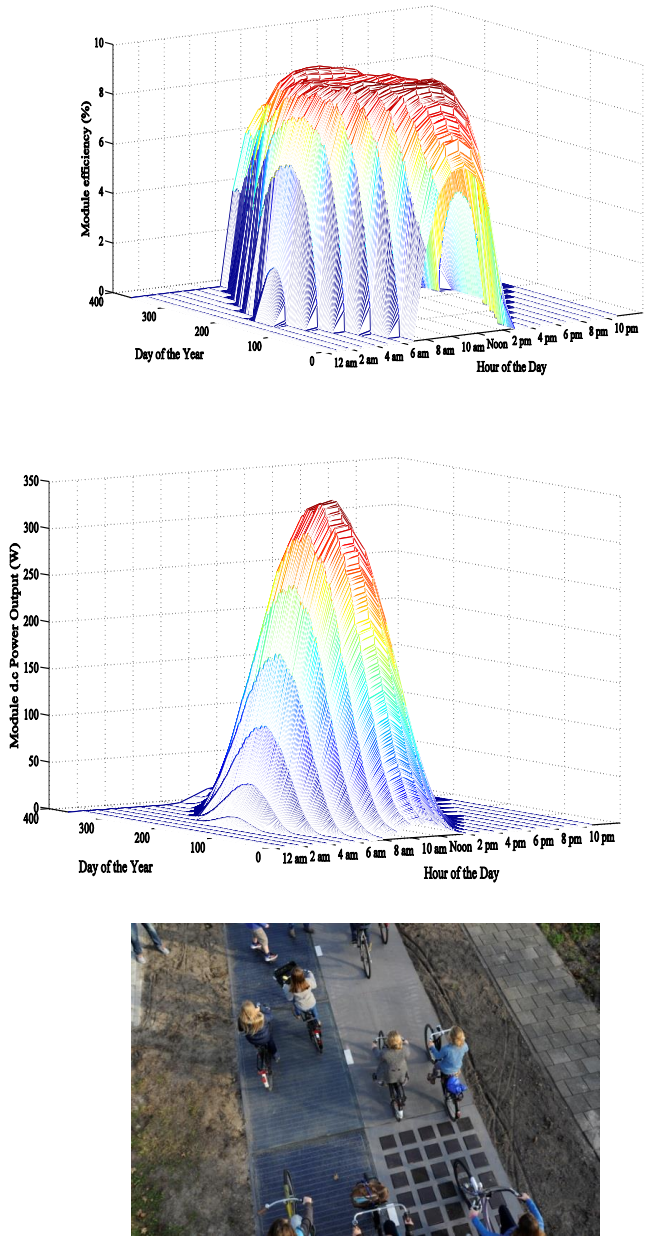

Fig. 5. Estimated Operating Efficiency of the Solar Road in Year 2015, estimated dc power output in the same year and installed Solaroads in the bike lane in the village of Krommenie, North Holland [12].

The practical problem with applying this self-healing property to heal roads is that the self-healing process at ambient temperature is too slow to heal the asphalt in between the periods of no stress. The healing rate of the asphalt concrete will increase at higher temperatures [15]. The heating can be done using different methods, but induction heating is preferred over other methods, because it does not contaminate the asphalt, can provide a good distribution of the heating power inside the asphalt and it is possible to properly control the amount of heat generated [16]. For the asphalt to be heated by means of induction it first needs to be conductive, so eddy currents can be induced in the asphalt. This is achieved by mixing additives in the asphalt, like graphite or steel wool. Asphalt which is treated with such additives will be referred to further on as inductive healing asphalt. A description of induction heating for self-healing is indicated in Fig. 6.

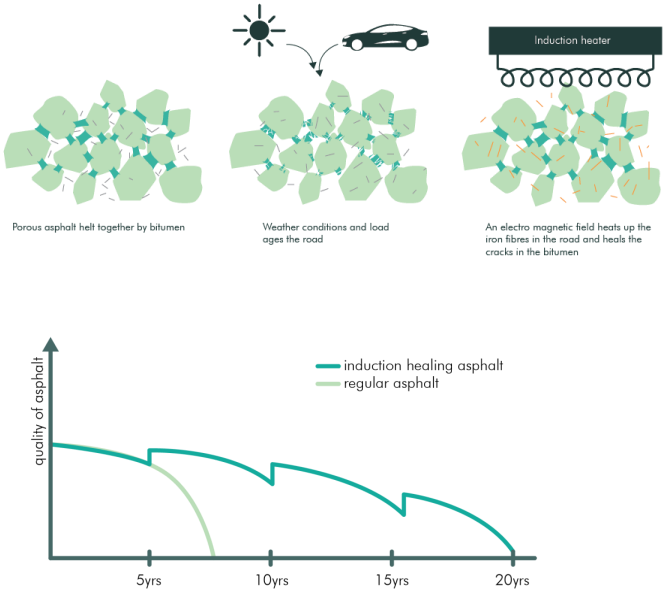

Fig. 6. The process of induction heating of self-healing roads and the resulting increase in life span of the roads.

II. Case Study- Design for an Inductively Powered Highway A12

The A12 motorway in the Netherlands (165 km) is an important highway that connects the city of Hague to the city of Arnhem. This case study involves the dynamic IPT coverage and sizing of renewable energy sources close to this highway. Some assumptions and constraints of this study are:

- A single EV - Nissan LEAF with a battery of 24 kWh is assumed to make a complete trip.
- Such an EV with a small battery presents a worst case scenario for Dutch highway interms of IPT coil installation. A detailed costing for IPT systems on buses is presented in [17].
- The vehicle dynamics are simulated based on equations and assumptions in [8].
- The vehicle is assumed to begin the journey at 80% SOC and must finish with dynamic IPT links such that it completes the trip with its SOC$>=$ 20% (worst case SOC $=$ 20%).

- The dynamic charging power is 50 kW at 85% efficiency with the vehicle traveling urban roads at 60 km/h (beginning and fag end of the journey) and 110 km/h.
- The power demand of EVs in future Dutch highways and the renewable energy sizing is considered for the year 2030.

The total energy for completing the trip with assumed SOC change is presented in Table I.

TABLE I
ENERGY REQUIREMENT FOR NISSAN LEAF BETWEEN 20% - 80% SOC

Characteristic	SOC (%)	Battery Energy (kWh, 85% efficiency)
Total	100%	20.4
Start	80%	16.3
End	20%	4.1
Total energy	80 to 20%	12.2

Also, power demand at different speeds are estimated linearly as 24.1 kW for 120 km/h and 5.6 kW for 60 km/h. The total energy required for the velocity profile of the assumption is 31 kWh and is detailed in Table II.

TABLE II
ENERGY REQUIREMENT FOR NISSAN LEAF TO COMPLETE THE JOURNEY

Driving speed (km/h)	Travelled Distance (km)	Energy used (kWh)
60	10	0.9
120	34	6.8
120	20	4
120	31.7	6.4
120	30	5.9
120	29.3	5.9
60	10	0.9
Total	165	31.0

Incorporating the vehicle speed limits, the energy in different sections are also presented. Hence, the total power demand from dynamic IPT is $31.0 - 12.2 = 18.8$ kWh. With a 50 kW inverter with a transfer energy of 85%, the power transferred is 42.5 kW. The time needed to transfer this energy is $18.8/42.5 = 0.44$ h. At a driving speed of 120 km/h, the charging distance is 53 km. At a speed of 110 km/h this distance is 49 km. A distance of 50 km is chosen, this is a road coverage of $50/165 = 30.3\%$. This road coverage was then distributed over busiest parts of the highway. This resulted in two IPT charge areas of 20 km (area A) and 30 km (area B) respectively.

The result of estimated SOC for these assumptions for both EVs with and without IPT charging is shown in Fig. 7.

This graph shows both vehicles starting with a SOC of 80%. The vehicle with on-road IPT reaches its destination with a SOC of $20-25\%$, while the other vehicle without on-road IPT needs to recharge at charging stations. This distance seems to be sufficient to drive between 20% and 80% of the battery SOC while reaching the destination. Also, Fig. 8 shows the effect of different average velocities on the driving range of the vehicle.

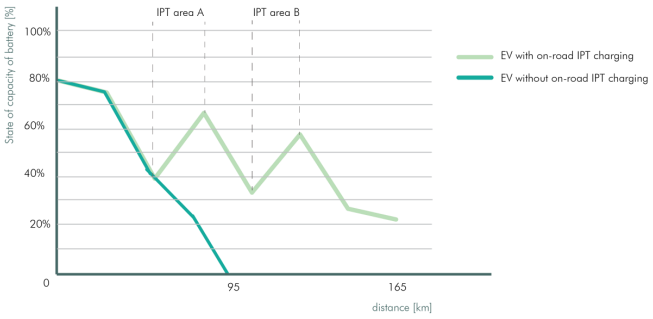

Fig. 7. State of capacity for a journey with and without on-road IPT, analyzed at average speed = 120 km/h. The electric vehicle with on-road IPT reaches its destination with a SOC of 20% while the other vehicle does not reach its destination and needs to stop for charging. The electric vehicle with on-road IPT is charged at two locations during its journey.

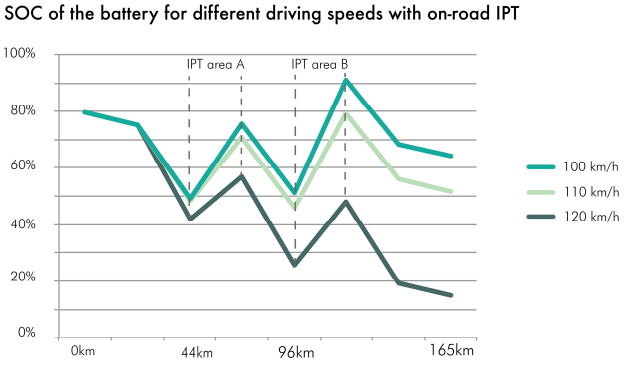

Fig. 8. The state of capacity of the battery for three different average driving speeds on the highway. The average speed for urban driving remained the same for all three situations. An average driving speed of 100km/h is much more energy efficient.

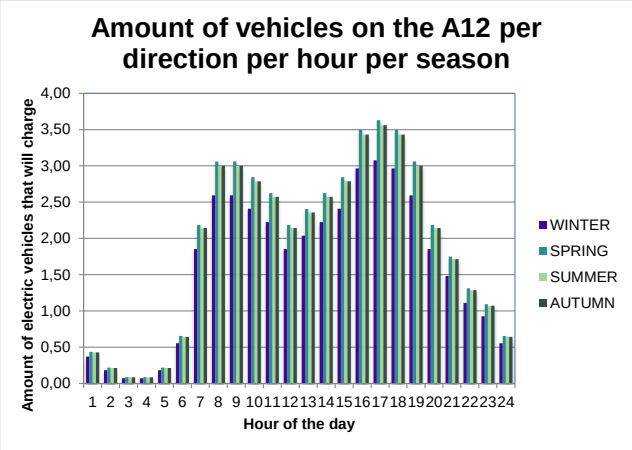

Fig. 9. Seasonal dependence of number of EVs per hour per direction.

A. Sizing renewable energy sources for 2030

1) EV power requirement: The highway A12 due to the traffic requirement, contains two charge areas of 20 km and

30 km. Both areas are powered with a 50 kW IPT system. In 2030, 2.3 million electric vehicles are expected in the Netherlands while 8 million gasoline vehicles will exist [19]. Roughly, in 2030 about 40% of all vehicles will be electric.

For calculations on the power demand, it is assumed that 10% of all traffic will charge while driving. Based on the measurements of the A12, Fig. 9 is created from [20] on the traffic intensity. The graph shows the total number of EV per km per hour in one direction of the journey. This corresponds to an IPT power profile as shown in Fig. 10.

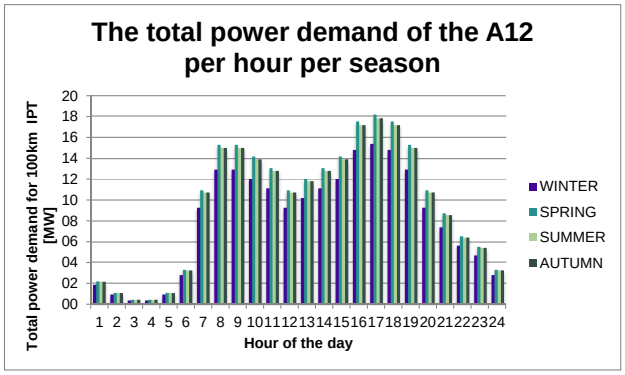

Fig. 10. Seasonal dependence of power demand of EVs per hour for a round trip.

2) Solaroad emergency lane: The expectation of solar panels along the noise barrier was not feasible, as power input is below 10% of the total energy output of solar energy sources. Thus, solaroads along the emergency lanes produce the solar electricity. The total length of these lanes on the A12 is 114 km (considering lack of in some sections). The surface of this lane is 114 km $\times$ 3.15 m $=$ 399000 m^2. The solar irradiance per month per hour is visible in Fig. 11.

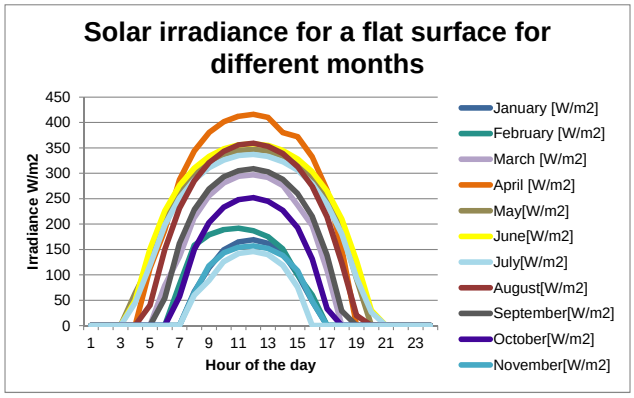

Fig. 11. Solar irradiance for a horizontal flat surface during a whole year in A 12 [18].

The efficiency of the solaroad is 9.69 %. In winter the panels provide no power at 17.00 h. This figure also shows the average insolation per season to visualize a clear difference between each season. Also, the total power generated by the solaroads is presented in Fig. 12.

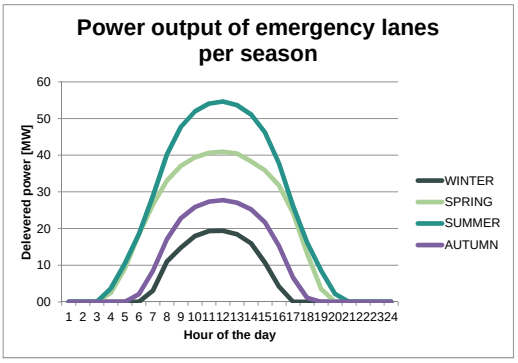

Fig. 12. Power delivery of the solaroad emergency lanes on the A12 per hour per season.

3) Wind power: The wind speeds per season per hour at 80 m height is retrieved from the weather station Cabauw, which is located close to the A12. The wind profile along the A 12 is not very divergent along its length [22]. The profile is indicated in Fig. 13.

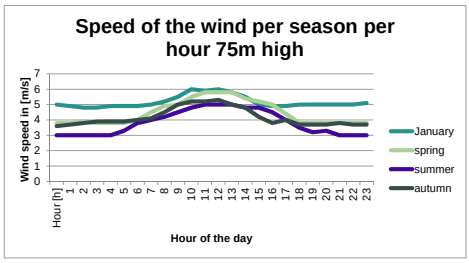

Fig. 13. Speed of the wind per season per hour at 80m height at forecast station Cabauw, Netherlands [21].

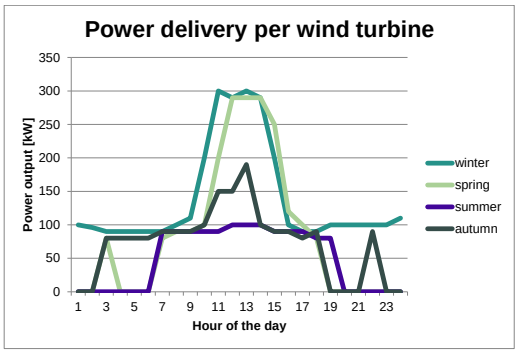

Fig. 14. Power output of one wind turbine per hour per season in the Netherlands, Cabauw.

The power delivered by a 2 MW wind turbine per season per hour is presented in Fig. 14. When the speed of the wind

is below 4 m/s the power output is assumed to be 0 W. In case of vortex, a 4 kW vortex, 13 m high is used to estimate the performance. The wind speeds were scaled using an on-line tool. The performance curve in Fig. 4 is used to convert the wind speeds to output power as in Fig. 15.

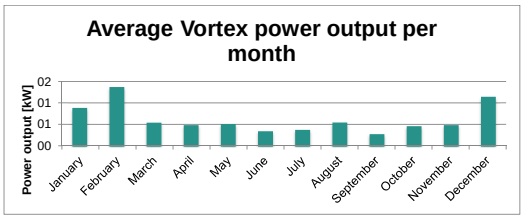

Fig. 15. Average power output per month for a single Vortex.

The amount of solar energy from the Solaroad on the emergency lanes is taken as a constant and is calculated for the maximum coverage possible. The amount of Vortex and wind turbines needed to provide the remaining required power demand also depends on the costs and other benefits of both products. In Fig. 16, the total power output per day per month of the renewable energy sources is visualized.

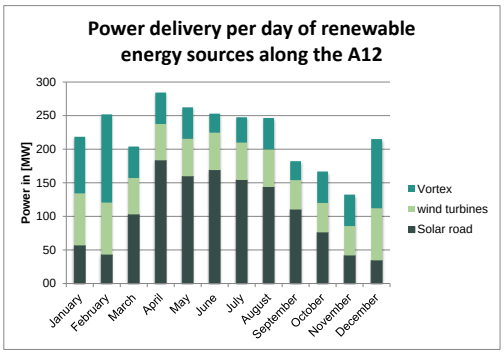

Fig. 16. Power delivery to the 100km IPT track on the A12. Both emergency lanes are replaced with a solaroad and 50% of the wind power is generated by Vortex and the other 50% of the wind power is generated by wind turbines.

As presented, the Solaroad has the highest contribution in spring and summer. While in autumn and winter, it is wind energy. The wind energy mix between conventional turbine and vortex is 50%:50%.

4) Matching power demands: In Fig. 17, the daily power demand from the grid is visible. The demand from the grid is positive visualized; the generation of renewable energy is indicated with a negative value. From midnight until 6 : 00 h, the grid receives energy. For spring and summer, the grid is sourced more energy compared to autumn and winter. This also counts for the middle of the day. The power demand on the grid in the morning and afternoon is small compared to the daily grid power demand; the highest peak is 15 MW at 14 : 00 h. The remaining green energy can be transferred to the grid or to nearby residents or offices to store the energy in electric vehicles.

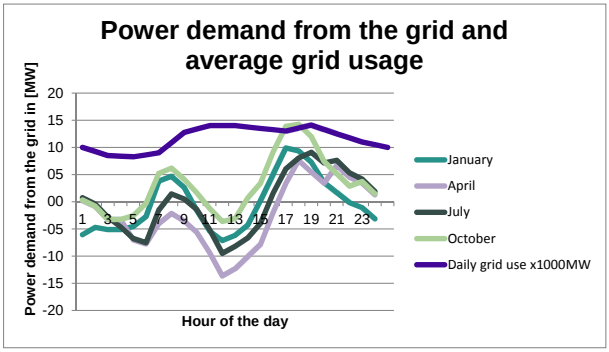

Fig. 17. The power demand from the grid by the IPT system per season is presented by a positive value. Two peaks are visible in the morning and afternoon when traffic density is highest. During the night and in the middle of the day the grid receives energy. The average grid use is scaled down in order to create a clear visual graph [23].

Fig. 18 shows the amount of Nissan Leafs that can be charged per hour. Since these vehicles will be parked at home or at the office the vehicles will charge on a normal charging rate.

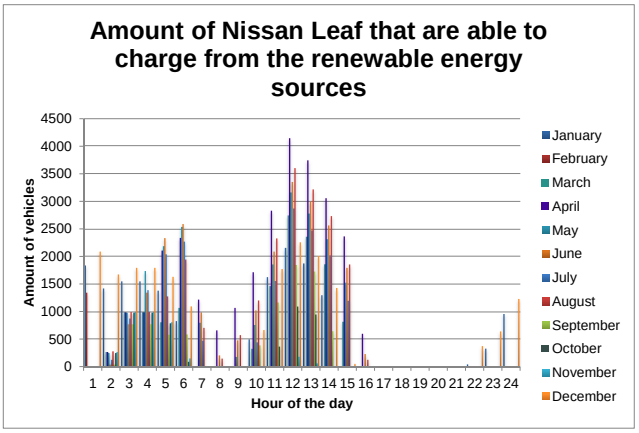

Fig. 18. The amount of Nissan Leaf that can be charged per hour by the power output from the renewable energy sources, which is not used for IPT charging.

III. Combination of IPT with Inductive Healing Asphalt

Induction heating is often implemented with high frequency coils, which is also the primary source of power in most IPT systems. Therefore there is potential to combine the two. The challenge is to enable the system to switch between IPT to the EVs & between the induction heating of asphalt. For the design, priority is that the losses are minimized in asphalt with IPT, which can be significant.

A regular IPT equivalent circuit was expanded with complex inductances of the form $L = L_r - jR_L$ that will model hysteresis and eddy current losses [24], [25] as shown in Fig. 19, in order to compare the losses in the self-healing asphalt and its performance capabilities with air cored IPT system. The impedance

of such an inductance L will be $Z_L = \omega R_L + j\omega L_r$, which can also be modelled using a resistance and an inductance.

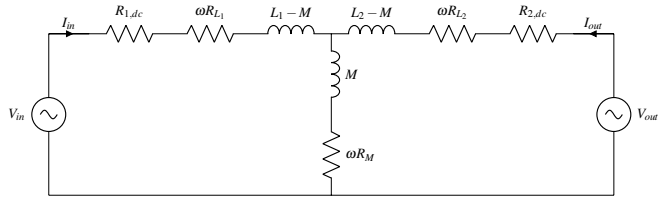

Fig. 19. Inductive power transfer circuit with eddy current and hysteresis losses in the inductive healing asphalt.

The linear system describing the model becomes

$$V = \begin{bmatrix} R_{1,dc} + \omega R_{L_1} & \omega R_M \\ \omega R_M & R_{2,dc} + \omega R_{L_2} \end{bmatrix} I + j\omega \begin{bmatrix} L_1 & M \\ M & L_2 \end{bmatrix} I \quad (1)$$

The circuit parameters for the linear system of (1) can be extracted using COMSOL Multiphysics 5.1. A 2D axis-symmetrical system with a planar primary copper coil of 23 turns, wire radius of 0.25 mm, an inner & outer radius of 25 mm and 105 mm, respectively, the secondary coil being identical, as shown in Fig. 20.

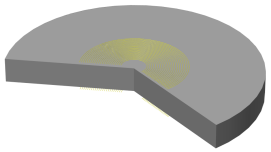

Fig. 20. Sketch of FEM model used to extract the circuit parameters.

The vertical distance between the coils and the asphalt layer is 5 mm. The radius of the asphalt layer is 250 mm and the thickness is varied between 10 mm, 50 mm and 100 mm. For each coil the parameters are extracted using the emf phasor $\mathscr{E}$, the current phasor I and the real power P from the simulations. The induced emf in the coils of the system is given by

$$\mathscr{E} = j\omega \begin{bmatrix} L_1 & M \\ M & L_2 \end{bmatrix} I. \quad (2)$$

Using this equation the complex inductances for the system can be determined. First the self inductance of the primary coil L_1 will be calculated by exciting the coil while the secondary is simulated as an open circuit. Then the secondary coil is simulated as a short circuit while the excitation of the primary remains the same. Using the previously calculated self inductance of the primary the mutual inductance M between the primary and the secondary can be calculated. This is then done again the other way around to determine the value of L_2.

The coil dc resistances are calculated from the current through the coils and the power P dissipated in the copper of the coils.

The IPT system with the layer of inductive healing asphalt in between is compared to an air core IPT system of the same dimensions which simulates the case when there is regular non-magnetic and non-conductive asphalt. The inductive healing asphalt is modelled as a homogeneous material with a conductivity of $\sigma = 500$ [S/m] and a relative permeability of $\mu_r = 4$ [26]. The comparison is done by means of the maximum output power and the coupling factor. The maximum output power is calculated using the maximum apparent power, which is defined as

$$S_{out,max} = V_{out,oc} \times I^*_{out,sc}, \quad (3)$$

where $V_{out,oc}$ is the open circuit output voltage and $I_{out,sc}$ is the short circuit output current. For the maximum output apparent power it is assumed that there is a unity power factor in the input and the output, thus that both of the leakage inductances are compensated for by resonant capacitances. The expression for the maximum output apparent power then becomes

$$\begin{aligned} V_{out,oc} &= (\omega R_M + j\omega M) I_{in} \\ I_{out,sc} &= \frac{(\omega R_M + j\omega M)}{R_{2,dc} + \omega R_{L_2}} I_{in} \\ S_{out,max} &= \frac{\omega R_M^2 + \omega^2 M^2}{R_{2,dc} + \omega R_{L_2}} I_{in}^2. \end{aligned} \quad (4)$$

It should be noted that there is no imaginary part in the expression for the maximum apparent power, and thus it is equal to the maximum output power which gives $P_{out,max} = S_{out,max}$. The minimum input power for that particular I_1 is equal to the output power plus the losses in the primary.

$$P_{in,min} = (R_{1,dc} + \omega R_{L_1}) I_{in}^2 + P_{out,max} \quad (5)$$

The maximum efficiency can now be calculated as $\eta_{max} = \frac{P_{out,max}}{P_{in,min}}$ resulting in

$$\eta_{max} = \frac{\omega R_M^2 + \omega^2 M^2}{(R_{1,dc} + \omega R_{L_1})(R_{2,dc} + \omega R_{L_2}) + \omega R_M^2 + \omega^2 M^2}. \quad (6)$$

It should be noted that this is a theoretical maximum efficiency which will never be reached in any practical setup, so it should be seen as a upper boundary. The coupling factor of the systems ($k = \frac{M}{\sqrt{L_1 L_2}}$) will be compared.

A. Results of combined IPT and Self-Healing roads

The maximum efficiency and the coupling factor between the primary and the secondary were investigated over a range of frequencies from 1 kHz to 10 MHz. This was done for three different asphalt layer thicknesses of 1 cm, 5 cm and 10 cm. In Fig. 21, the coupling factor is presented. In the range of 1 kHz - 10 kHz, the coupling factor of the system with inductive healing asphalt is approximately constant. In this range, the coupling with 1 cm of inductive healing asphalt is decreased to 69% of the air core system. For the other two cases it reduces to below 50%. At higher frequencies, due to skin effect, the mutual inductance drops which further decreases coupling.

It is clear in Fig. 22, that the maximal efficiency dramatically drops when the asphalt layer is 5 cm or 10 cm thus it is not feasible to combine IPT and inductive healing asphalt without modifications. With the method that is described above it is easy to compare various concepts that can increase the efficiency and coupling of IPT and inductive healing asphalt combined systems. Currently additional studies are

being performed to increase the performance of the combined system to achieve a feasible efficiency of IPT.

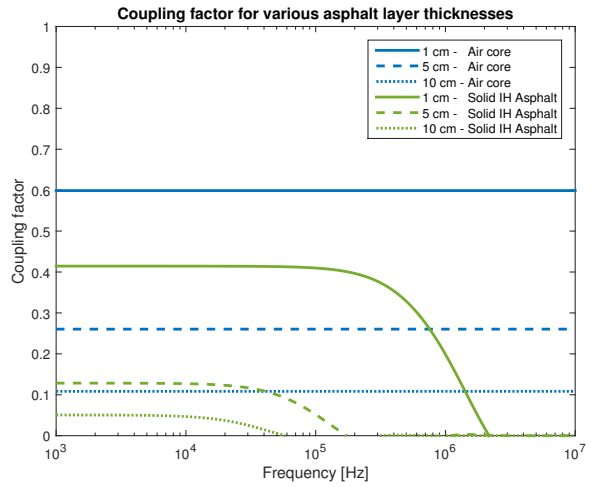

Fig. 21. Coupling factor of the primary and the secondary coil with a varying thickness of the asphalt layer for a wide range of frequencies.

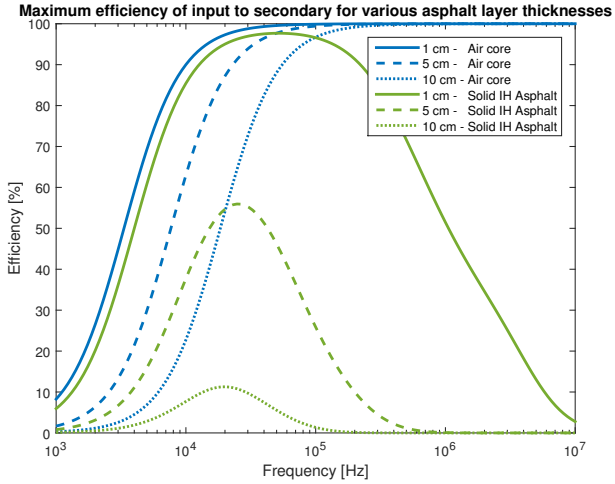

Fig. 22. Maximum IPT efficiency of input to secondary with a varying thickness of the asphalt layer for a wide range of frequencies.

IV. Conclusion

It is possible for an EV to complete its trip 80% -20% SOC along A12 by on-road IPT system. The total IPT coverage (IPT efficiency = 85%) in this highway is 30.3%. This corresponds to a distance of 50 km in a highway of total length 165 km.

Applying solar panels on the noise barriers doesn't yield large energy returns. The Solaroads along emergency lanes for 114 km at efficiency of 9.7% yields a peak afternoon power of 55 kW in Summer. However, during winter, no power is produced from 17 : 00 h - 6 : 30h.

The solar and wind energy complement each other by having peaks in summer and spring on the one hand and in winter and autumn in the other.

A detailed sizing for vortex and wind turbines also involve cost, which is not considered in this study and will be considered in a future work. The addition of self-healing asphalt to improve the longevity of roads will result in losses in the same during IPT mode. A solution that can curtail losses is considered for future work.

References

[1] F. Fan and Y. Lei, "Decomposition analysis of energy-related carbon emissions from the transportation sector in Beijing," *Transportation Research Part D: Transport and Environment*, vol. 42, 2016.

[2] "Reducing Transport Greenhouse Gas Emissions Trends & Data," 2010. [Online]. Available: http://www.internationaltransportforum.org

[3] N. Lutsey, "global climate change mitigation potential from a transition to electric vehicles," 2015.

[4] T. Litman, "Autonomous Vehicle Implementation Predictions: Implications for Transport Planning," *Transportation Research Board Annual Meeting*, vol. 42, no. January 2014, pp. 36–42, 2014.

[5] D. Milakis, M. Snelder, B. Van Arem, G. Van Wee, and G. Homem De Almeida Rodriguez Correia, "Exploring plausible futures of automated vehicles in the netherlands: results from a scenario analysis," 2015.

[6] V. Prasanth and P. Bauer, "Distributed ipt systems for dynamic powering: misalignment analysis," *Industrial Electronics, IEEE Transactions on*, vol. 61, no. 11, pp. 6013–6021, 2014.

[7] G. A. Covic and J. T. Boys, "Inductive power transfer," *Proceedings of the IEEE*, vol. 101, no. 6, pp. 1276–1289, June 2013.

[8] T.-E. Stamati and P. Bauer, "On-road charging of electric vehicles," in *Transportation Electrification Conference and Expo (ITEC), 2013 IEEE*. IEEE, 2013, pp. 1–8.

[9] Bladeless vortex. [Online]. Available: http://www.vortexbladeless.com/

[10] Solaroad. [Online]. Available: http://en.solaroad.nl/

[11] Bladeless wind turbines may offer more form than function. [Online]. Available: https://www.technologyreview.com

[12] A. Shekhar, S. Klerks, P. Bauer, and V. Prasanth, "Solar road operating efficiency and energy yield – an integrated approach towards inductive power transfer," in *European Photovoltaic Solar Energy Conference and Exhibition (EU-PVSEC)*, 2015, pp. 2614–2619.

[13] J. L. M. Voskuilen and P. N. W. Verhoef, "Cause of premature raveling failure of porous asphalt." *Sixth international RILEM symposium on performance testing and evaluation of bituminous materials*, 2003.

[14] "Induction heating of electrically conductive porous asphalt concrete," *Construction and Building Materials*, vol. 24, no. 7, 2010.

[15] B. Kim and R. Roque, "Evaluation of healing property of asphalt mixtures," *Transportation Research Record: Journal of the Transportation Research Board*, vol. 1970, pp. 84–91, 2006.

[16] Q. Liu, "Induction healing of porous asphalt concrete," Ph.D. dissertation, TU Delft, October 2012.

[17] A. Shekhar, V. Prasanth, P. Bauer, and M. Bolech, "Economic Viability Study of an On-Road Wireless Charging System with a Generic Driving Range Estimation Method," *Energies*, vol. 9, no. 2, 2016.

[18] Photovoltaic geographical information system - interactive maps. [Online]. Available: http://re.jrc.ec.europa.eu/pvgis/apps4/pvest.php#

[19] "Een duurzame brandstofvisie met lef, ministerie van infrastructuur en milieu," 2014.

[20] Verkeer 2010 - maarsbergen. afdeling planvorming en advies droog (wvp). [Online]. Available: https://www.rijksoverheid.nl

[21] T. E. Stamati and P. Bauer, "Green energy for on-road charging of electric vehicles," in *MECHATRONIKA, 2012 15th International Symposium*, Dec 2012, pp. 1–9.

[22] "Windkaart van nederland op 100 m hoogte," 2014.

[23] Electricity consumption netherlands. [Online]. Available: http://www.tennet.eu

[24] D. C. Meeker, E. H. Maslen, and M. D. Noh, "A wide bandwidth model for the electrical impedance of magnetic bearings," in *Third International Symposium on Magnetic Suspension Technology*, vol. 2, June 1996.

[25] D. Buecherl, H. G. Herzog, "Iron loss modeling by complex inductances for steady state simulation of electrical machines," in *SPEEDAM*, 2010.

[26] P. Apostolidis, "Experimental and numerical investigation of induction heating in asphalt mixes," Master's thesis, TU Delft, November 2015.